

Electrolyte Management for Effective Long-Term Electro-Osmotic Transport in Low-Permeability Soils

NERINE J. CHEREPY*

Chemistry and Materials Science Directorate, Lawrence Livermore National Laboratory, Livermore, California 94550

DORTHE WILDENSCHILD†

Energy and Environment Directorate, Lawrence Livermore National Laboratory, Livermore, California 94550

Electro-osmosis, a coupled-flow phenomenon in which an applied electrical potential gradient drives water flow, may be used to induce water flow through fine-grained sediments. Test cell measurements of electro-osmotic transport in clayey cores extracted from the 27–31 m depth range of the Lawrence Livermore National Laboratory site indicate the importance of pH control within the anode and cathode reservoirs. In our first experiment, pH was not controlled. As a result, carbonate precipitation and metals precipitation occurred near the cathode end of the core, with acidification near the anode. The combination of these acid and base reactions led to the decline of electro-osmotic flow by a factor of 2 in less than one pore volume. In a second experiment, long-term water transport (>21 pore volumes) at stable electro-osmotic conductivity ($k_{eo} \sim 1 \times 10^{-9} \text{ m}^2/\text{s}-\text{V}$) was effected with anode reservoir pH > 8, and cathode reservoir pH < 6. Hydraulic conductivity (k_h) of the same core was $4 \times 10^{-10} \text{ m/s}$ under a 0.07 MPa hydraulic gradient without electro-osmosis. Stable electro-osmotic flow was measured at a velocity of $4 \times 10^{-7} \text{ m/s}$ under a 4 V/cm voltage gradient, and no hydraulic gradient—3 orders of magnitude greater than the hydraulic flow. We also observed chloroform production in the anode reservoir, resulting from electrochemical production of chlorine gas reacting with trace organics. The chloroform was transported electro-osmotically to the cathode, without measurable loss to adsorption, volatilization, or degradation.

Introduction

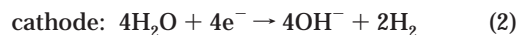
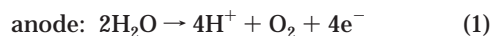
Fine-grained sediments contaminated with organic solvents are pollution sources, slowly diffusing dissolved contaminants into adjacent high-permeability zones, leading to groundwater contamination. Since hydraulic pumping in a heterogeneous matrix draws water primarily through the coarse-grained zones, circumventing finer-grained zones with higher contamination, mechanical pump-and-treat technology is not effective in the cleanup of clayey, fine-grained zones. We are therefore exploring the use of in-situ electro-osmotic pumping to flush contaminants from fine-grained sediments (1–3).

* Corresponding author phone: (925)424-3492; fax: (925)422-0049; e-mail: cherepy1@llnl.gov.

† Current addresses: Environment & Resources, Technical University of Denmark, 2800 Lyngby, Denmark and Department of Geosciences, Oregon State University, Corvallis, OR 97333.

Electro-osmotic pumping of water is a well-known technology with applications in structural engineering for soil stabilization (4), mining (5), and remediation (6–10). Electromigration, electro-osmosis, and electrophoresis are collectively referred to as electrokinetics (11). Electrokinetic soil remediation technology employs electrodes placed in the ground with a direct current (DC) passed between them using an external power supply. A good recent review of electrokinetic remediation, describing many recent technological innovations, has been published by Virkutyte and co-workers (12). Electromigration may be used for removal of metal contaminants, such as lead, cadmium, and copper (8, 10, 12, 13). Electro-osmosis is a secondary effect arising from electromigration of cations through the porous matrix under an applied electrical potential. Clays have a net negative surface charge, balanced in the Helmholtz double layer by exchangeable cations. The flow of current results in movement of these cations and their associated water of hydration from anode to cathode, entraining contaminants, if present in the pore water, in the flow. Thus, electro-osmotic pumping can increase well yield in fine-grained sediments 2–3 orders of magnitude over flow rates achievable by hydraulic pumping alone. Electro-osmotic pumping technology offers great potential for controlled cleanup of fine-grained sediments, since flow follows the domain of the imposed electric field and passes preferentially through fine-grained sediments due to their greater electrical conductivities. It is an in-situ technology, requiring no excavation.

Electrolysis reactions at the anode and cathode result in the water splitting reactions:



Other electrochemical reactions may occur, depending on the species present in the electrode reservoirs. For example, Cl_2 may be formed at the anode from Cl^- .

We present work investigating the management of electrolyte pH to prevent progressive decline in electro-osmotic flow rates. For electrokinetic metal removal, standard methodology utilizes controlled pH shifts, entraining the acid generated from water electrolysis at the anode in the electrokinetic flow to desorb metals and keep them solubilized for removal from the clay surface (7, 10, 12–15). In contrast, our work aims to remediate organics from soils, and therefore we are exploring the use and management of electro-osmotic processing fluids that maintain stable anode-to-cathode flow and controlled pH. Some earlier evidence suggested that pH control of anode water in the neutral to basic range promotes flow (16, 17), and acid addition to the cathode helps to control carbonate and hydroxide precipitation reactions in the vicinity of the cathode (14, 18). Reduction in flow rates due to precipitate formation has been reported and addressed using buffers (8), continuous rinsing of the cathode (19), and chelating agents such as EDTA (20). Ion exchange membranes may be a good solution, as described by Ottosen and co-workers (10) and by Li et al. (21), but they are somewhat difficult to implement in the field due to their fragility and lifetime (22). In addition, acidification of the soil still occurs under typical implementation conditions, which favors solubilization and removal of metals, but leads to instability of the soil. Further, these membranes typically exhibit low permeability to the larger organic contaminants. For the application to removal of organics, avoidance of any

pH gradients is desirable to allow long-term electro-osmotic flushing without affecting the matrix.

We also explore the use of electro-osmosis to transport volatile organics through low-permeable sediments to remove it from the contaminated groundwater zone at the Lawrence Livermore National Laboratory (LLNL) site. Several studies of electro-osmotic removal of polar aromatic compounds have been reported. Combined contaminants, metals, and polycyclic aromatic hydrocarbons were removed via electrokinetic transport in a series of laboratory experiments by Maini et al. (14). In this case, electro-osmotic transport of these slightly soluble organics (90% removal) was much more significant than the electromigration of toxic metals, even with no surfactants. Similarly, phenol and pentachlorophenol were removed at 85% efficiency with electro-osmotic water flushing by Kim et al. (18). Li and co-workers demonstrated the use of cosolvents to efficiently mobilize phenanthrene (23). Ko et al. reported enhanced electrokinetic phenanthrene removal using a cyclodextrin complexing agent, which may be a more promising mobilization approach than detergents, which adsorb to clay surfaces (24).

We are particularly interested in the transport and removal of chlorinated solvents. Several projects studying the transport of weakly polar volatile chlorinated solvents with electro-osmosis have been attempted previously (25, 26). Reactive barriers using zerovalent iron for removal of halogenated species are well-known (27). The Lasagna Project at the Paducah Gaseous Diffusion Plant demonstrated electro-osmotic transport of trichloroethylene through reactive barriers (carbon, iron filings) resulting in removal rates of up to 99% (6). Rohrs and co-workers demonstrated up to 80% removal of chlorinated butadiene, butenes, and butanes within the soil matrix, but without evidence of transport. They assert that the contaminants were degraded, possibly with catalysis by naturally occurring conductive metal oxides, aided by high pH and reducing conditions. This raises the possibility that transport of contaminants out of the soil may not be necessary for their degradation and removal (28).

Experimental Section

We have designed and built two functionally equivalent test cells to measure hydraulic and electro-osmotic flow, hydraulic gradient, electrical current, and voltage distributions. Test Cell 2 was built to avoid problems with corrosion and difficult assembly encountered with Test Cell 1. With these benchtop cells, we made measurements of hydraulic (k_h) and electro-osmotic (k_{eo}) conductivities of a soil core during the progress of electro-osmotic treatment. Hydraulic conductivity, k_h , is obtained using Darcy's Law

$$k_h = \frac{q_h L}{HA} \quad (3)$$

where q_h is the hydraulic flux, L is the length of the core, H is the hydraulic pressure gradient, and A is the cross-sectional area of the core. The electro-osmotic conductivity, k_{eo} , is calculated using

$$k_{eo} = \frac{q_{eo} L}{EA} \quad (4)$$

where q_{eo} is the electro-osmotic flux, L is the length of the core, and E is the voltage drop.

For both cells, a 0–50 V Hewlett-Packard 6633B power supply was employed in DC constant voltage mode for electro-osmotic transport experiments. Water was supplied to the anode side of the cell by a standpipe during electro-osmotic flow measurements and by a pressurized water vessel for hydraulic flow measurements. Gases generated

TABLE 1. Typical Characteristics of LLNL Groundwater Used for Experiments

parameter	value
total Ca	88 mg/L
total Mg	38 mg/L
total Na	124 mg/L
total K	1.2 mg/L
PO ₄ ³⁻	0.2 mg/L
Cl ⁻	137 mg/L
SO ₄ ²⁻	46 mg/L
NO ₃ ⁻	5.4 mg/L
SiO ₂	30 mg/L
pH	8.0
electrical conductivity (25 °C)	100 μmhos/cm

via electrolysis were free to escape through the standpipes. The water used for all experiments was LLNL site groundwater, obtained from the on-site treatment facility after filtration with granular activated carbon (for removal of organic contaminants), with no added chlorine or other adulterants. Typical major ion concentrations of this water are shown in Table 1. Two narrow diameter standpipes, outfitted with 0–1.25 psi (0–8618 Pa) pressure transducers (Validyne DP 215-50), were used to measure water inflow and outflow.

Test Cell 1. In Test Cell 1, in-situ conditions were simulated by subjecting the sample to a confining pressure matching the underground stresses of the original location of the soil core. The core used in Test Cell 1 for the measurements reported here was extracted using an auger drill from the 36.4–36.6 m depth of a well drilled for a field installation at Treatment Facility F at LLNL. In this area, the water table lies at 29 m, and the stresses on the core can thus be estimated to lie in the 0.21–0.42 MPa range. Therefore, all Test Cell 1 measurements were acquired with confining pressure of 30 psi (0.21 MPa). However, subsequent studies of the effect of varying confining pressure (5–30 psi) on flow rates showed it to be negligible, beyond the requirement that water not flow in the annular region between the core and the Teflon sleeve.

Test Cell 1 (Figure 1a) consists of a pressure vessel holding a 8.9 cm diameter × 15.2 cm long soil core (Figure 1b) with a porosity measured via pycnometry of ~30% (pore volume 283 mL). The core diameter was defined by the drill and was cut to the cell length. The core was jacketed using a heat gun with a heat-shrink Teflon sleeve (TexLoc FEP roll cover) to seal against the confining pressure and to avoid short-circuiting of the water flow at the circumference of the sample. Two perforated gold plated copper electrodes (anode and cathode) were placed on each end of the sample, and gold wire hoops were placed around the core, approximately 5 cm from each electrode, for use as voltage probes (Figure 1c). These wires were jacketed in Teflon sleeves to allow feedthrough and accurate voltage measurements of the zone in electrical contact with the hoops only. The gold-plated diffusion plates were used to transfer the applied longitudinal load to the sample as well as serving as electrodes. They were separated from the soil by a microporous membrane (Pall-RAI Electropore E40201 ultrahigh MW polyethylene, 100 μm thick, 2 μm pores). All electrical contacts were made with gold wire.

A constant DC voltage of 45.72 V (3 V/cm gradient) was supplied to the gold-plated endplates, adjacent to the ends of the core, during electro-osmotic processing. Current densities were in the 1.5–2.5 mA/cm² range, decreasing during treatment. No reagents were added for pH control, and pH of both the anode and cathode reservoirs did not drift significantly from neutral. Both hydraulic and electro-osmotic conductivity measurements were performed alter-

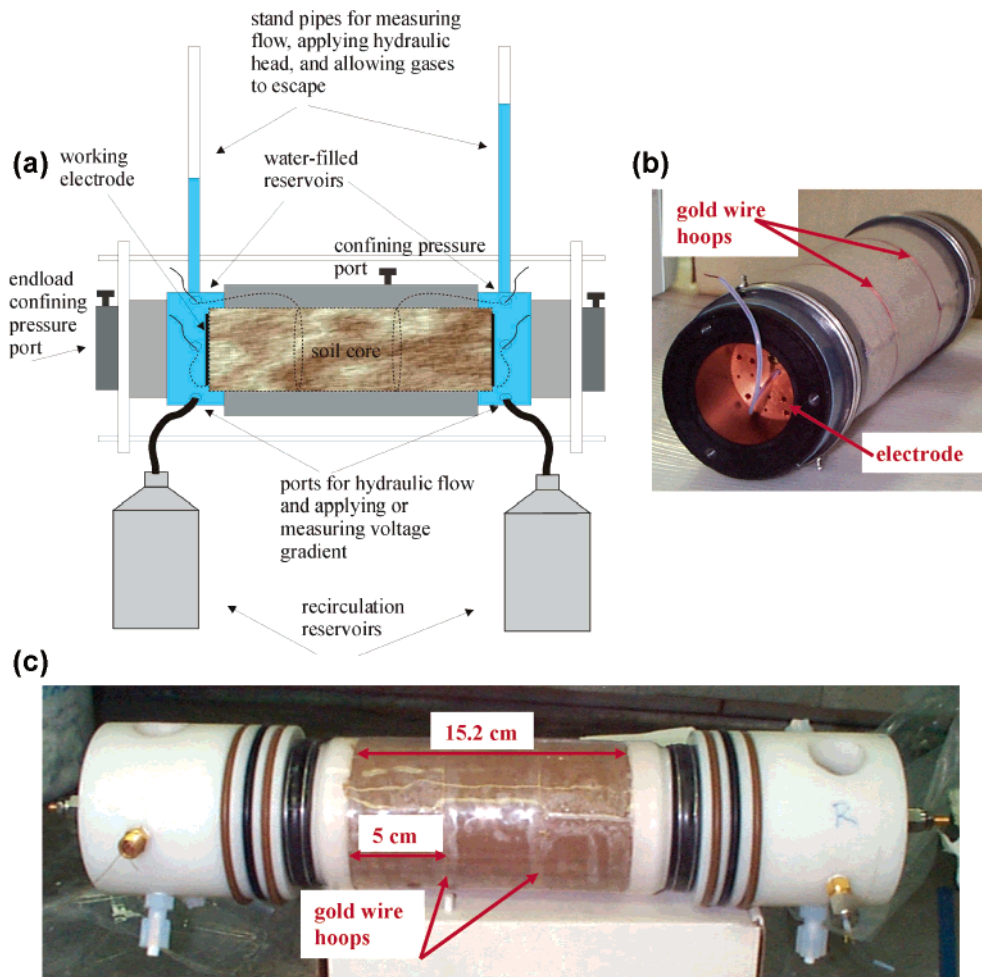


FIGURE 1. a. Test Cell 1. The core is contained within the central pressure vessel, and water flow is measured as the level rises in the right-hand (cathode) standpipe. b. Core assembly for Test Cell 1. The core is jacketed in Teflon shrink-wrap, with gold-plated copper perforated electrodes at both ends, and two gold hoop voltage probes to provide information about the voltage drop along the core. c. Test Cell 1 core with white Delrin water reservoirs attached (steel confining pressure vessel not shown).

nately, of which 11 days of electro-osmotic processing were carried out (195 mL transported electro-osmotically).

Test Cell 2. A simpler cell was then built to allow rapid assembly/disassembly, to minimize corrosion, and to allow visual access to the core (Figure 2). The core was 6.35 cm diameter (due to a different drilling rig) and 7.62 cm long and was also jacketed in a Teflon sleeve, attached to endpieces containing the microporous membrane/voltage probe assembly and compressed with throughbolts (not shown) and a strong-back to avoid short-circuiting of water flow in hydraulic conductivity mode. Working electrodes in Cell 2 were Ebonex conductive titanium oxide ceramic disks (Electrosynthesis Inc.), 5.08 cm diameter, suspended in Lucite electrode reservoirs 5 cm from the core on either side. The water in each electrode reservoir was constantly mixed via peristaltic pump with a volume of 4.2 L contained in an external reservoir. This idea of mixing with an external reservoir has been described by others, as well (10, 14, 15, 18). Pall RAI microporous membranes separated titanium mesh (Exmet) voltage probes placed at either end from the core, and titanium wires were used for all electrical connections.

The core was extracted from the 28.5–29.0 m zone of Treatment Facility D at LLNL. Its soil composition was nearly identical to that used in Cell 1. For this core, one pore volume was estimated at 72 mL. It was hydraulically saturated with water for several pore volumes. Electro-osmotic pumping was initiated with a power supply at a constant voltage of 50

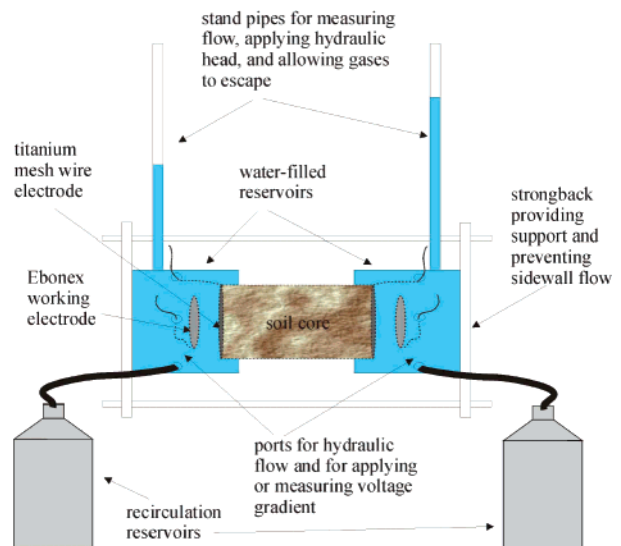


FIGURE 2. Test Cell 2. The core is jacketed in Teflon shrink-wrap, with titanium mesh voltage probes at either end. Water flow is measured as the level rises in the cathode standpipe. The Ebonex working electrodes were suspended in the water reservoir 5 cm from the core.

V for the duration of experiments, current density ranged from 3.5 to 8.9 mA/cm², increasing during processing. This

TABLE 2. Characteristics of Soil Core Used in Test Cell 1 before Experiment

parameter	value
porosity	~30%
sand	68%
silt	11%
clay	21%
carbonate	1.34%
K	126 ppm
Mg	473 ppm
Ca	1759 ppm
Na	118 ppm
cation exchange capacity	1.35 mequiv/100 g
total organic carbon	1.9 ppm

current density is higher than that for the Cell 1 experiments due to the shorter length of the core used in Cell 2 and possibly the more thorough hydraulic saturation of the Cell 2 core. A 3 V/cm gradient was used for Cell 1, while a 6.57 V/cm gradient was used with Cell 2. The anode reservoir was "over-controlled" to pH > 8, and the cathode reservoir was over-controlled to pH < 6 in a closed recirculation system, using KOH and HCl. These pH values were not constant and varied at the anode from pH 8 to 11 and at the cathode from 3 to 6. Electro-osmotic flow continued for a total of 31 days, including overnight during the week. This corresponds to a total of 1518 mL of water transported (21.1 pore volumes).

Analytical Methods. Water samples for chlorinated hydrocarbon analyses were collected in 3 mL vials, filling completely to avoid headspace, chilled on ice, and analyzed within 12 h using a modified EPA Method 601 (29). Measurements of soil properties, typical for the cores used in both Test Cell 1 and Test Cell 2, were carried out by A&L Western Labs, Modesto, CA. For Test Cell 2, post-treatment anolyte and catholyte chemical analyses were performed by BC Labs, Bakersfield, CA.

Results and Discussion

The cores chosen for work in the benchtop cell were selected due to their high clay content, representative of the finer-grained Flayers in the screened zone of the wells drilled for electro-osmotic remediation field installations (3). Typical soil characteristics for the cores used in these experiments are shown in Table 2. The hydraulic conductivity measured for these cores is indicative of the type of sediments we are interested in targeting for cleanup with electro-osmotic pumping but would not necessarily be typical of a measurement between wells in a field installation. The soil cores used in test cell experiments are small, isolated from natural hydraulic gradients, and represent the finer-grained zones of a natural heterogeneous fabric.

The two experiments reported herein represent the extremes of treatment methodologies, and each taken separately would lead to dramatically different conclusions about the usefulness and applicability of electro-osmotic pumping as a remediation technology. The Test Cell 1 experiment shows some of the limitations of this technology, while the Test Cell 2 experiment demonstrates that when implemented correctly, electro-osmotic pumping may be used as a long-term pump-and-treat technology for contaminants requiring extraction of many pore volumes for their effective removal.

Test Cell 1. Electrodes Adjacent to Core, No pH Control.

In Test Cell 1, the voltage imposed between the anode and cathode (at either end of the 15.2 cm long soil core) was controlled in constant voltage mode. The measured current was linear with voltage. Further detail about the voltage drop along the core was provided by two supplemental gold hoop voltage probes at 5 and 10 cm along the core, and the voltage

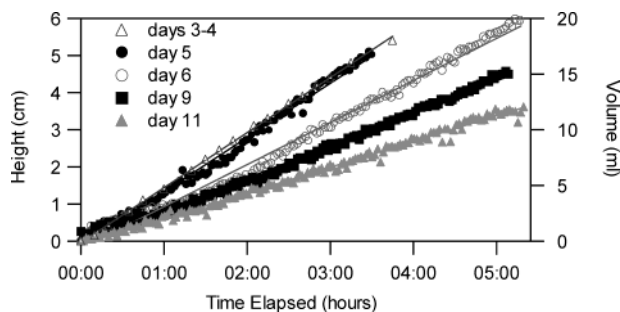


FIGURE 3. The electro-osmotic flow in Test Cell 1 using a 3 V/cm voltage gradient.

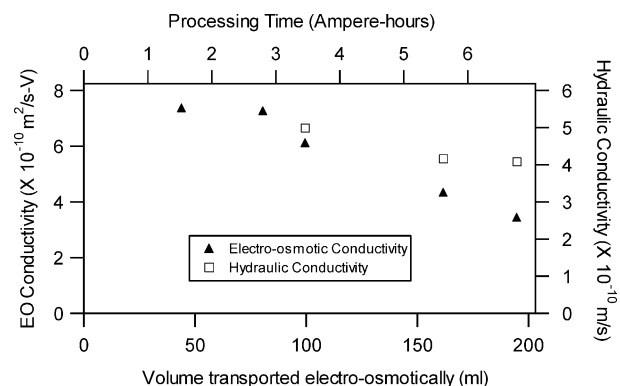


FIGURE 4. The electro-osmotic and hydraulic conductivities of the Test Cell 1 core both decreased during processing. Electro-osmotic conductivity declined by ~2 \times , while the decline in hydraulic conductivity was slight, ~1.2 \times less. The volume transported electro-osmotically, 195 mL, is 0.7 pore volumes.

drop between the hoops was also linear with current. We measured a soil electrical conductivity of 0.090 S/m on day 1, decreasing to 0.071 S/m at the end of processing on day 11.

Electro-osmotic conductivity (k_{eo}) measurements were performed under controlled conditions in the benchtop cell. Five measurements taken during electro-osmotic processing are presented in Figure 3. A 3 V/cm applied voltage resulted in a $q_{eo} = 0.082$ mL/min on day 3, decreasing to 0.038 mL/min on day 11. The electro-osmotic conductivity for the 8.9 cm diameter core calculated from these measurements declined from $k_{eo} = 7.4 \times 10^{-10}$ to 3.4×10^{-10} m²/s-V after 11 days of processing (Figure 4).

Hydraulic conductivity was measured for the core in Test Cell 1 using a pressure differential imposed by a pressurized water reservoir on the inlet side and a standpipe open to atmospheric pressure at the outlet side. Initial flow rate using a pressure gradient of 10 psi (0.069 MPa) was 0.0085 mL/min. This corresponds to a hydraulic conductivity for this core of $k_h = 5.0 \times 10^{-10}$ m/s, and repeated measurements of the hydraulic conductivity did not indicate significant changes during treatment, the final k_h measured being 4.1×10^{-10} m/s (Figure 4). Sediments with hydraulic conductivities in this range may be considered essentially impermeable to mechanical pumping, especially when interleaving sandy layers ($k_h > 10^{-6}$ m/s) are present.

In summary, for Test Cell 1, in which electrodes were next to the core, and no efforts to control pH were carried out, we measured declines in the electrical, hydraulic, and electro-osmotic conductivity of a clayey core in a benchtop test cell during electro-osmotic processing in conjunction with precipitation within the core. No significant changes in pH were measured in the reservoirs, since the H⁺ and OH⁻ fronts were drawn into the core electrokinetically, toward the cathode and anode, respectively. Metals, including

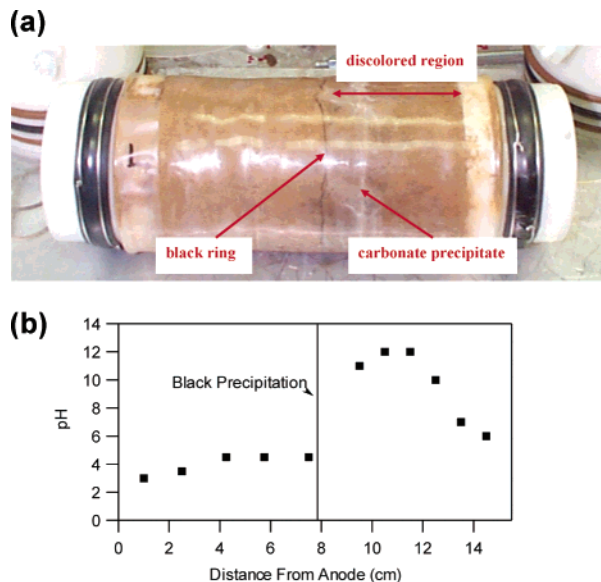


FIGURE 5. a. Test Cell 1 core at the end of electro-osmotic processing. Discoloring is seen in a zone close to the cathode (right end), with a distinct black ring at the furthest left portion of the discolored area. The black metals deposition and white carbonate precipitate occurred at the outer perimeter of the core. b. Distribution of pH along the length of the Test Cell 1 core. The anode is at the left end of the core and the cathode at the right end. The pH rises sharply at the precipitation zone.

corrosion products from the gold-plated copper anode, as well as metals naturally present in the soil, such as calcium, were solubilized in the acid front propagating from the anode and formed a black precipitate upon meeting the OH^- front propagating from the cathode, the principal component being copper oxide (Figure 5). In addition, where the base penetrated the core, carbonates precipitated. This precipitation zone developed closer to the cathode end, due to the lower mobility of OH^- (self-diffusion coefficient $D_0 = 52.8 \times 10^{-10} \text{ m}^2/\text{s}$) relative to H^+ ($D_0 = 93.1 \times 10^{-10} \text{ m}^2/\text{s}$) (1). The cause of loss of electro-osmotic conductivity is likely a combination of the acidification of the anode end of the core and consequent loss of cation exchange capacity as well as lowered local permeability in the area of mineral precipitation. These results led us to develop Test Cell 2 in which the electrodes were suspended in the water reservoirs to facilitate pH control and prevent the acid/base fronts from penetrating into the soil.

Test Cell 2. Electrodes Suspended in pH-Controlled Reservoir. In Test Cell 2, the voltage imposed between the anode and cathode (electrodes in the reservoirs) was also controlled in constant voltage mode. The current measured in the system varied linearly as a function of the voltage applied to the electrodes varied between 0 and 50 V. Likewise, the current had a linear dependence on the voltage drop measured with the titanium voltage probes at either end of the core. The voltage drop in the system was measured at the start of the experiment to be linear, and the voltage drop along the core, measured with two supplemental titanium mesh voltage probes pressed against the microporous membrane at either end of the core, was also linear with current. The electrical conductivity of the core at start of experiments was 0.255 S/m. This is considerably more electrically conductive than the core studied in Test Cell 1, probably because this core had been thoroughly saturated hydraulically prior to the electro-osmosis experiment. Figure 6 shows the voltage drop across the core rose from ~ 15 to ~ 30 V during the run (voltage gradient ~ 2 V/cm to ~ 4 V/cm, respectively), and the current rose from ~ 18 mA to ~ 40 mA.

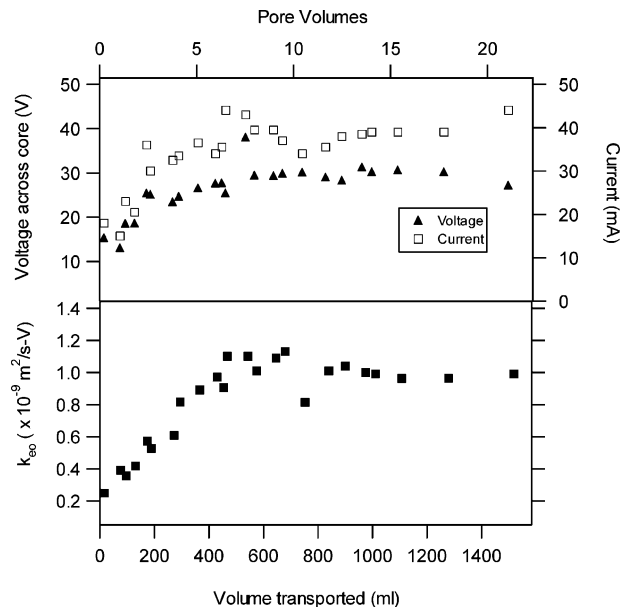


FIGURE 6. Test Cell 2 experiment. Top: The voltage drop across the core rose from ~ 15 to ~ 30 V during the run (voltage gradient ~ 2 V/cm to ~ 4 V/cm, respectively), and the current rose from ~ 18 mA to ~ 40 mA. Bottom: The electro-osmotic conductivity (k_{eo}) improved early in the experiment. Once reaching $k_{eo} = 1 \times 10^{-9} \text{ m}^2/\text{s-V}$, at ~ 6 pore volumes, the electro-osmotic conductivity remained stable for the duration of the experiment.

The hydraulic conductivity measured during the saturation of the core with groundwater was $4.2 \times 10^{-10} \text{ m/s}$, at an 8 psi (0.055 MPa) hydraulic gradient. At the end of experimentation, the hydraulic conductivity of the core was measured with a pressure gradient of 10 psi (0.069 MPa) to be $3.8 \times 10^{-10} \text{ m/s}$ (flow rate of 0.4 mL/h). This dense clay was very similar to the core used in Test Cell 1 and would be essentially impermeable to hydraulic pumping for field work where clayey zones are not isolated but lie above or below more permeable zones.

The electro-osmotic conductivity (k_{eo}) improved early in the experiment, probably due to the increased electrical conductivity of the pore water and reservoir water as acid and base neutralizing reagents were added. Once reaching $k_{eo} = 1 \times 10^{-9} \text{ m}^2/\text{s-V}$, at ~ 6 pore volumes (at about 400 mL) the electro-osmotic conductivity remained stable for the duration of experiments (Figure 6). This corresponds to an effective hydraulic velocity (or flux) of $4 \times 10^{-7} \text{ m/s}$ at 4 V/cm, 3 orders of magnitude greater than the hydraulic velocity (measured at a hydraulic gradient of 0.069 MPa) with no electro-osmosis.

The results of this experiment are markedly different from those of Test Cell 1. No pH gradient formed within the core, and measurements taken upon disassembly showed neutral pH throughout the core. No precipitation occurred within the core, and not only did the electro-osmotic conductivity not decline with treatment time but it improved. These results are very strong evidence for the importance of pH control. The use of noncorroding electrodes also minimized the transport of metal cations into the core, and the hydraulic presaturation of the core may have helped increase its electrical conductivity. It is important to note that the presence of high levels of carbonates in the soil and water used in these experiments also help buffer acidification at the anode. Also, the closed reservoirs at the anode and cathode provide conditions of increasing ionic conductivity with treatment time. Results would no doubt be quite different for conditions in which the catholyte and anolyte are continuously exchanged out for low conductivity water

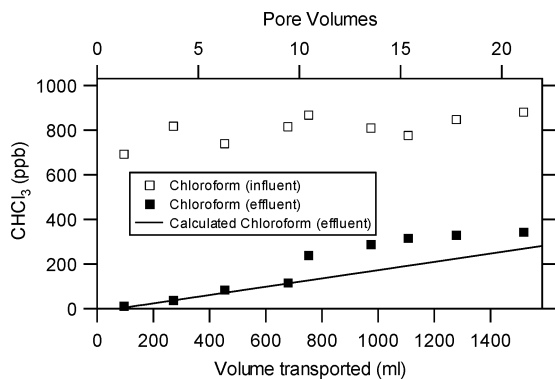


FIGURE 7. CHCl_3 concentration was stable at ~ 800 ppb in the influent anode reservoir (open symbols) and showed transport into the effluent cathode reservoir (closed symbols) via electro-osmotic transport. The calculated CHCl_3 level (solid line) is based on dilution of volume transported into the cathode reservoir, where the effluent reservoir was held at 4400 ± 100 mL for the duration of the experiment.

(such as a soil zone below the water table), resulting over time in deionization via electromigration of the treatment zone. Thus, the present results are more applicable to shallow treatment zones than to the deeply buried zones from which the cores were extracted.

A concern regarding mineral precipitation on the cathode surface led us to carry out experiments (not shown here) in which periodic voltage reversal results in dissolution of carbonates, "cleaning" the cathode. However, for the experiments shown here in Test Cell 2, no voltage reversal was ever done, and at the end of the experiment the cathode was completely coated with calcium carbonate. The resistivity of this film was apparently more than offset by the increased conductivity of the catholyte over time, as measured by the voltage drop between the cathode and the titanium mesh voltage probe at the cathode end of the core, which declined steadily during treatment.

The measurement of production of chloroform (CHCl_3) in the anode reservoir and its transport via electro-osmosis to the cathode reservoir demonstrates the utility of this technology for removal of dissolved nonpolar organics. This observation is in line with a previous report of tests at Point Magu of halomethane production at the anode (30). This deserves consideration, as a new pollutant is being formed by the treatment process. It is very important to note, however, that the use of a different acid in the catholyte than HCl might significantly alleviate the formation of chlorinated byproducts. In any case, in soils with naturally high chloride content, the formation of Cl_2 at the anode and subsequent byproducts is unavoidable, as shown in the Point Magu studies where citric acid was used at the cathode (30). In addition to CHCl_3 , we detected bromodichloromethane, bromoform, chloromethane, and dibromochloromethane in the catholyte at the end of experimentation, but at much lower levels, 1–50 ppb. The concentration of dissolved CHCl_3 studied was low, however, compared to contaminated sites, and it remains to be seen how electro-osmosis might work for mobilization of dense nonaqueous phase liquids present in clayey zones.

The CHCl_3 concentration measured during the course of electro-osmotic treatment in the influent and effluent (Figure 7) was found to be approximately constant in the influent (anode) compartment, at ~ 800 ppb, rising in the effluent compartment from 12 to 343 ppb over the duration of the experiments. This is an effective demonstration of the advection of a weakly polar volatile chlorinated solvent through a soil core via electro-osmosis. If hydraulic gradient-induced flow were responsible for the transport it would have required approximately 1098 days (assuming a maxi-

TABLE 3. Characteristics of Anolyte and Catholyte from Test Cell 2, after Experiment

parameter	value (anolyte)	value (catholyte)
total Ca	20 mg/L	320 mg/L
total Mg	15 mg/L	100 mg/L
total Na	26 mg/L	240 mg/L
total K	1100 mg/L	3200 mg/L
total Al	7 mg/L	11 mg/L
NO_3^-	35 mg/L	9.9 mg/L
pH	8.6	3.4
electrical conductivity (25 °C)	3590 $\mu\text{mhos/cm}$	14600 $\mu\text{mhos/cm}$
total dissolved solids	2460 mg/L	10200 mg/L

imum gradient between standpipes of 100 cm) to transport the ~ 1500 mL through the core. A simple calculation of progressive transport of the anode water (800 ppb in CHCl_3) into the cathode (0 ppb in CHCl_3 until the first pore volume has been transported) following

$$[\text{CHCl}_3]_{\text{eff}} = [\text{CHCl}_3]_{\text{in}} * \frac{V_{\text{tr}}}{V_{\text{res}}} \quad (5)$$

where $[\text{CHCl}_3]_{\text{eff}}$ and $[\text{CHCl}_3]_{\text{in}}$ are the effluent and influent chloroform concentrations, V_{tr} is the volume transported from the influent into the effluent, and V_{res} is the fixed (4400 ± 100 mL) volume in the effluent electrode reservoir, external reservoir, standpipe, and tubing assembly. The data roughly match the calculation. No significant loss of CHCl_3 was observed due to volatilization, adsorption within the soil matrix, or degradation. The lack of adsorption is likely due to the low organic content in this relatively deeply buried zone, shown in Table 2, TOC of 1.9 ppm.

We had considered that we might observe degradation of CHCl_3 in the vicinity of the cathode. Electrochemical degradation of chlorinated hydrocarbons has reportedly been facilitated by conductive oxides naturally present in soil (29) or with reactive iron filings zones (6, 31) for catalysis. The possibilities for combining electro-osmotic transport with reductive chlorination open up some very efficient removal and treatment strategies, taking advantage of the hydrogen "byproduct" and coupling it to an efficient catalyst, such as platinum (32).

The water from the anode reservoir (anolyte) and the cathode reservoir (catholyte) were analyzed for ionic concentrations upon termination of the experiment with Test Cell 2 (Table 3). The anolyte pH of 8.6 and the catholyte pH of 3.4 are typical of the over-controlled pH regime used throughout treatment. Calcium, magnesium, sodium, and potassium concentrations are about an order of magnitude greater in the catholyte than in the anolyte. Significantly higher cationic concentrations in the catholyte results from metals removal from the soil core. The one anion measured, nitrate, was at ~ 3 times higher concentration in the anolyte, as would be expected based on its expected electromigration.

We have shown that electro-osmotic transport can be used to facilitate water flow and dissolved chlorinated solvents, if present, in natural sediments. Control of pH is required for long-term operation in a system such as our benchtop test cells, in which electro-osmosis was studied in the absence of hydraulic gradients and three-dimensional mixing. Significant issues involved with field installations, including the difficulty of controlling and extracting mobilized contaminants in the presence of background hydraulic flow, may present further challenges to field implementation of electro-osmotic pumping.

The original aspects of this work include the following: (1) measurement of hydraulic as well as electro-osmotic flow rates and conductivities of real soil cores, (2) clear demon-

stration of the poor outcome of lack of pH control and a corroding anode, (3) demonstration of very long-term flow (>21 pore volumes) with the use of Ebonex electrodes and over-controlled pH in electrode reservoirs, (4) measurement of a steady-state production of chloroform in the anode reservoir and its lossless transport to the cathode, with implications for removal of organics from contaminated sediments.

We measured typical electro-osmotic flow velocities of $\sim 4 \times 10^{-7}$ m/s for a core with hydraulic conductivity of $\sim 4 \times 10^{-10}$ m/s. The cost of electricity to move water via electro-osmosis is small (0.5–2 kWh/L, ~ 5 –20¢/L), rather, the greatest costs arise from the capital investment in equipment, siting, and maintenance. Electro-osmotic flushing could provide the basis for a pump-and-treat technology for fine-grained zones, and its application to the LLNL site has already shown promise for adaptation to removal of chlorinated solvents under the constraints of complex subsurface geology (3).

Acknowledgments

We are grateful to Allen Elsholz for his assistance with cell assembly, core handling, and experimental setup. Thanks to Walt McNab for helpful discussions, David Ruddle and Roberto Ruiz for cell design and fabrication, and Ken Carroll for analytical support. This work was performed under the auspices of the U.S. Department of Energy by University of California Lawrence Livermore National Laboratory under contract No. W-7405-Eng-48.

Literature Cited

- (1) Cherepy, N.; McNab, W.; Wildenschild, D.; Ruiz, R.; Elsholz, A. *Proc. Electrochem. Soc.: Environ. Aspects Electrochem. Technol.* **1999**, 99–39, 97.
- (2) Cherepy, N.; Wildenschild, D.; Elsholz, A. *Proc. Battelle Intl. Conf. Remediation Chlorinated Recalcitrant Compds.* **2000**, 2(5), 277.
- (3) McNab, W. W.; Ruiz, R. *Ground Water Mon. Remed.* **2001**, 21, 133.
- (4) Casagrande, L. *Geotechnique* **1949**, 1, 159.
- (5) Lockhart, N. C. *Int. J. Miner. Process.* **1983**, 10, 131.
- (6) Ho, S. V.; Athmer, C.; Sheridan, P. W.; Hughes, B. M.; Orth, R.; McKenzie, D.; Brodsky, P. H.; Shapiro, A. M.; Thornton, R.; Salvo, J.; Schultz, D.; Landis, R.; Griffith, R.; Shoemaker, S. *Environ. Sci. Technol.* **1999**, 33, 1086.
- (7) Acar, Y. B.; Gale, R. J.; Alshawabkeh, A. N.; Marks, R. E.; Puppala, S.; Bricka, M.; Parker, R. *J. Hazard. Mater.* **1995**, 40, 117.

- (8) Lageman, R. *Environ. Sci. Technol.* **1993**, 27, 2648.
- (9) Probst, R. F.; Hicks, R. E. *Science* **1993**, 260, 498.
- (10) Ottosen, L. M.; Hansen, H. K.; Saurisen, S.; Villumsen, A. *Environ. Sci. Technol.* **1997**, 31, 1711.
- (11) Mitchell, J. K. *Fundamentals of Soil Behavior*; John Wiley and Sons: New York, 1993.
- (12) Virkutyte, J.; Sillanpaa, M.; Latostenmaa, P. *Sci. Tot. Environ.* **2002**, 289, 97.
- (13) Eykholt, G. R.; Daniel, D. E. J. *Geotech. Eng. ASCE* **1994**, 120, 797.
- (14) Maini, G.; Sharman, A. K.; Knowles, C. J.; Sunderland, G.; Jackman, S. A. *J. Chem. Technol. Biotechnol.* **2000**, 75, 657.
- (15) Lee, H.-H.; Yang, J.-W. *J. Hazard. Mater.* **2000**, B77, 227.
- (16) Dzenitis, J. M. *J. Electrochem. Soc.* **1997**, 144, 1317.
- (17) Schultz, D. S. *J. Hazard. Mater.* **1997**, 55, 81.
- (18) Kim, S.-O.; Moon, S.-H.; Kim, K.-W. *Environ. Tech.* **2000**, 21, 417.
- (19) Hicks, R. E.; Tondorf, S. *Environ. Sci. Technol.* **1994**, 28, 2203.
- (20) Yeung, A. T.; Hsu, C.-N.; Menon, R. M. *J. Geotech. Eng. ASCE* **1996**, 122, 666.
- (21) Li, A.; Yu, J.-W.; Neretnieks, I. *Environ. Sci. Technol.* **1998**, 323, 394.
- (22) Unpublished results from field work at LLNL.
- (23) Li, A.; Cheung, K. A.; Reddy, K. R. *J. Environ. Eng. ASCE* **2000**, 126, 527.
- (24) Ko, S.-O.; Schlautman, M. A.; Carraway, E. R. *Environ. Sci. Technol.* **2000**, 34, 1535.
- (25) Segall, B. A.; O'Bannon, C. E.; Matthias, J. A. *J. Geotech. Engin. ASCE* **1980**, GT10, 1150.
- (26) Bruell, C. J.; Segall, B. A.; Walsh, M. T. *J. Environ. Eng. ASCE* **1992**, 118, 68.
- (27) Tratnyek, P. G. *Chem. Ind.* **1996**, 1 July, 499.
- (28) Rohrs, J.; Ludwig, G.; Rahner, D. *Electrochim. Acta* **2002**, 47, 1405.
- (29) U.S. Environmental Protection Agency (EPA). *Guidelines for Establishing Test Procedures for the Analysis of Pollutants: 40 CFR 104.1 Part 136*; U.S. Government Printing Office; Washington, DC, 1986.
- (30) Hodko, D.; Rogers, T. D.; Magnuson, J. W.; Dillon, J.; Anderson, K. C.; Madigan, and M.; VanHyfte, J. *Final Report – In Situ Electrokinetic Remediation of Metal Contaminated Soils*; Report Number SFIM-AEC-ET-CR-99021; U.S. Army Environmental Center: 2000.
- (31) Yang, G. C. C.; Long, Y.-W. *J. Hazard. Mater.* **1999**, B69, 259.
- (32) McNab, W. W.; Ruiz, R.; Reinhard, M. *Environ. Sci. Technol.* **1999**, 34, 149.

Received for review August 26, 2002. Revised manuscript received March 26, 2003. Accepted April 11, 2003.

ES026095H